Computación y Sistemas Vol. 8 Núm. 4, pp. 317-333
© 2005, CIC-IPN, ISSN 1405-5546, Impreso en México

Quantifying Contrast Methods through Morphological Gradient

Métodos para Cuantificar el Contraste a través del Gradiente Morfológico

Jorge D. Mendiola-Santibañez [1], Iván R. Terol-Villalobos[2]

[1] Universidad Autónoma de Querétaro
Doctorado en Ingeniería, ,
76000, Querétaro, México
mendijor@uaq.mx
[2] CIDETEQ, S.C.,
Parque Tecnológico S/N, San Fandila-Pedro Escobedo, 76700,
Querétaro, México
famter@ciateq.net.mx

Article received on september 14, 2004; accepted on march 17, 2005

Abstract

In this work two quantifying contrast models are proposed. The first contrast measure method employs the concept denominated difference of contrast; while the second one takes in consideration the luminance gradient concept. These models allow the selection of the best parameters in a group of output images obtained from the application of the morphological toggle mappings with size criteria. These morphological transformations have the characteristic of modifying the output contrast based on some proximity criterion. In order to illustrate the performance of these quantifying contrast models, a number of images were processed and compared at pixel and partition level
Keywords: Contrast Measure, Toggle Mappings, Flat Zone, Partition, Visualization.

Resumen

En este trabajo son propuestos dos modelos para cuantificar el contraste. El primer método para evaluar el contraste emplea el concepto denominado diferencia de contraste, mientras que el segundo método toma en consideración el concepto de gradiente de la luminancia. Estos modelos permiten la selección del mejor parámetro en un grupo de imágenes de salida obtenidas a partir de la aplicación de los mapeos de contraste morfológicos con criterio de tamaño. Estas transformaciones morfológicas tienen la característica de modificar el contraste de salida basados en algún criterio de proximidad. Para ilustrar el comportamiento de estos modelos que permiten cuantificar el contraste, un número de imágenes fueron procesadas y comparadas tanto a nivel píxel como a nivel partición.
Palabras Clave: Medida de Contraste, Mapeos de Contraste, Zona Plana, Partición, Visualización

1 Introduction

In mathematical morphology the contrast enhancement is based on the morphological contrast mappings as described by Serra [17]. The main idea of these transformations is the comparison of each point of the original image with two patterns; subsequently, the nearest value with respect to the original image is selected. The first works related to the contrast theory were carried out by Meyer and Serra [13]. Indirectly, a special class of toggle mappings denominated morphological slope filters (MSF) were introduced by Terol–Villalobos [22], [23], [24]. Here a gradient criterion was used as a proximity criterion. Moreover, in [25] the flat zone concept on the partition was introduced in the numerical case and the morphological slope filters were defined as connected transformations. Once the basic flat zone operations were defined in the numerical case on the partition; the morphological toggle mappings were proposed as connected transformations by Mendiola and Terol [11], [12]. One important difference between the toggle mappings proposed by Serra [17] and those proposed by Mendiola and Terol [11][12] was that the size of the structuring element was considered as variable parameter in the primitives as well as in the proximity criterion. Hence a wide set of contrasted representations was obtained. However; this originates a problem related to the selection of the best parameters associated with the output images presenting a good visual contrast. So far several morphological contrast transformations have been mentioned, disregarding the improvement of the contrast from the point of view of visualization. In other words it is important to be able to measure or calculate the physical contrast in images in a way that it is representative of the apparent or perceived contrast. The contrast measure directly involves the luminance concept; however, it is hard to have a direct measure of this physical parameter in the images. For example, in the literature the Michelson and Weber contrast measures have been used as common physical models [8].

While numerous models based on the human visual system have been proposed, they are mostly concerned with predicting our ability to perceive basic geometric shapes and optical illusions. Few of these models work properly; meanly because the human visual system is enormously complex. It is difficult to design comprehensive models, and even more difficult to design experiments to validate their predictions. Nevertheless, there have been several attempts that have produced reasonable successful models. These include – and this list is far from being complete – Barten [3], Blommaert and Martens [5], Horn [7], Peli [15], and Stockham [21]. Most of these models are concerned with predicting visual effects such as contrast sensitivity [3], lightness induction/assimilation and border effects [5], and lightness determination [7], Peli [15] and Stockham [21]. In our case, the main purpose of introducing two morphological contrast methods is to have a contrast measure useful in the determination of the output images presenting an enhancement in the contrast from the point of view of visual contrast. In other words, we can say that if the best parameters are obtained when the images are processed by some enhancement transformation, then the selected output image will present an improvement in the contrast and therefore a good visual contrast. The first quantitative contrast measure introduced in this work uses the concept denominated difference of contrast, and the second one employs the luminance gradient concept [2]. The proposal of these models is also accompanied with a series of experimental images computed by the application of the morphological toggle mappings with size criteria. These output images were processed at pixel and on the partition level with the purpose of illustrating the performance of the contrast measure.

This paper is organized as follows. Section 2, briefly presents the morphological contrast mappings defined at partition and pixel level. In section 3, two quantitative contrast methods are introduced as the proposal of this work; in addition several examples showing the operation of these measure contrast methods will be presented.

2 Morphological Basic Transformations and Toggle Mappings

2.1 Morphological Basic Transformations

In mathematical morphology a transformation is a morphological filter if and only if it is increasing and idempotent.

The basic morphological filters at pixel level are the opening $\gamma_{\mu B}$ and closing $\varphi_{\mu B}$ by a structuring element μB, where B is the elementary structuring element (3x3 pixels in this work) containing the origin, $\hat{B}$ is its transposed ($\hat{B} = \{-x: x \in B\}$) and μ, a homothetic parameter. These transformations are expressed by:

$$\gamma_{\mu B}(f)(x) = \delta_{\mu \hat{B}}(\varepsilon_{\mu B}(f))(x) \text{ and } \varphi_{\mu B}(f)(x) = \varepsilon_{\mu \hat{B}}(\delta_{\mu B}(f))(x)$$

Where $\delta_{\mu B}$ and $\varepsilon_{\mu B}$ are the dilation and erosion, respectively, expressed by the equations:

$$\varepsilon_{\mu B}(f(x)) = \wedge\{ f(y); y \in \mu\hat{B}_x \} \text{ and } \delta_{\mu B}(f(x)) = \vee\{ f(y); y \in \mu\hat{B}_x \}$$

Where $\vee$ and $\wedge$ are the sup and inf operators. Once defined the morphological dilation and erosion, the morphological gradient, morphological internal gradient and morphological external gradient are defined as follows:

$$\text{grad}_{\mu B}(f)(x) = \delta_{\mu B}(f)(x) - \varepsilon_{\mu B}(f)(x) \quad (1)$$

$$\text{gradi}_{\mu B}(f)(x) = f(x) - \varepsilon_{\mu B} f(x)$$

$$\text{grade}_{\mu B}(f)(x) = \delta_{\mu B}(f)(x) - f(x) \quad (2)$$

Remark 1. Henceforth, the expression γ_{μ} , $\gamma_{\mu B}$ will be equivalent i.e. γ_{μ} , $= \gamma_{\mu B}$. The elementary structuring element B will be avoided. When the homothetic parameter μ=1, it will also be discarded, i.e. $\delta_{\mu B} = \delta_B = \delta$. By convention, when $\mu = 0$, the structuring element μB is a set composed by one point (the origin).

2.2 Connectivity

Serra [18] established connectivity by means of the concept of connected class.

Definition 1. A connected class **C** in $\wp(E)$ is a subset of $\wp(E)$ such that:

a) $\varnothing \in \mathbf{C}$ for all $x \in E$, $\{x\} \in \mathbf{C}$.
b) For each family C_i in **C**, $\cap_i C_i \neq \varnothing \Rightarrow \cup_i C_i \in \mathbf{C}$

Where $\wp(E)$ represents the set of all sets of E. An element of ***C*** is called a connected set. One equivalent definition to the connected class notion is the opening family expressed by the next theorem [18].

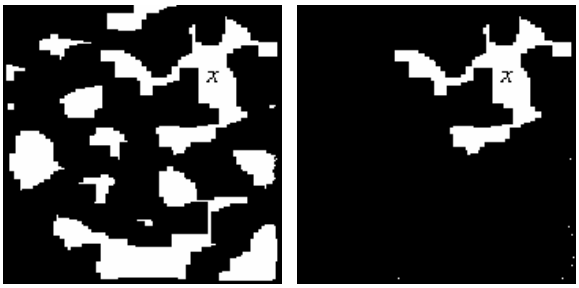

(a) (b)

Fig. 1. Connected components extraction (a) Binary image X, (b) The opening $\gamma_x(X)$ extracts the connected component in X where point x belongs

Theorem 1. (Connectivity characterized by openings). The definition of a connectivity class **C** is equivalent to the definition of a family of openings $\{\gamma_x , x \in E\}$ such that:
(a)$\forall$ $x \in E$, $\gamma_x(\{x\}) = \{x\}$
(b)$\forall$ $x,y \in E$ and $A \subset E$, $\gamma_x(A) = \gamma_y(A)$ or $\gamma_x(A) \cap \gamma_y(A) = \varnothing$
(c)$\forall$ $x \in E$ and $A \subset E$, $\forall$ $x \notin A \Rightarrow \gamma_x(A) = \varnothing$

When the transformation γ_x is associated to the usual connectivity (arcwise) in Z^2 (Z is the set of integers), the opening $\gamma_x(A)$ can be defined as the union of all paths containing x that are included in A. When a space is equipped with γ_x, the connectivity can be expressed using this operator. A set $A \subset Z^2$ is connected if and only if $\gamma_x(A) = A$. In Fig.1 the behavior of this opening is illustrated. The connected component of the input image X (Fig. 1(a)), where point x belongs, is the output of the opening $\gamma_x(X)$; while the other components are eliminated.

Definition 2. (Partition). Given a space E, a function $P: E \rightarrow \wp(E)$ is called a partition of E if: (a) $x \in P(x)$, $x \in E$, (b) $P(x) = P(y)$ or $P(x) \cap P(y) = \varnothing$ with $x, y \in E$.

P(x) is an element of the partition containing x. If there is a connectivity defined in E and; $\forall$ x, the component P(x) belongs to this connectivity, then the partition is connected.

Definition 3. The flat zones of a function $f: Z^2 \rightarrow Z$ are defined as the connected components (largest) of points with the same value of the function.

The operator $F_x(f)$ will represent the flat zone of a function f at point x.

Definition 4. An operator is connected if and only if it extends the flat zones of the input image.

Definition 5. Let x be a point of Z^2 equipped with γ_x . Two flat zones $F_x(f)$ and $F_y(f)$ in Z^2 are adjacent if: $F_x(f) \cap F_y(f) = \gamma_x (F_x(f) \cup F_y(f))$

Note that: (a) $x \in F_x(f)$, and (b) $\forall x, y$, $F_x(f) = F_y(f)$ or $F_x(f) \cap F_y(f) = \varnothing$. Therefore, the flat zone notion generates a partition of the image. Then, the use of both concepts, flat zone and partition were used for the introduction of morphological transformations in the gray level case.

Definition 6. Let x be a point in Z^2 equipped with γ_x. The set of flat zones adjacent to F_x is given by: $A_x = \{ F_{x'}(f): x' \in Z^2 , F_x(f) \cup F_{x'}(f) = \gamma_x (F_x(f) \cup F_{x'}(f))\}$.

In Fig. 2 the adjacent flat zone concept is illustrated; in Fig. 2(b) and 2(c) two adjacent flat zones are presented; while in Fig. 2(d) the adjacency of the expression $F_x(f) \cup F_y(f) = \gamma_x (F_x(f) \cup F_y(f))$ is illustrated.

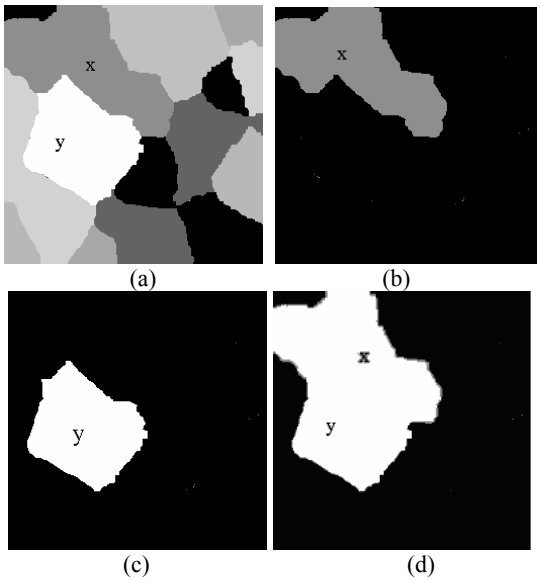

Fig. 2. (a) Image f with 14 flat zones; (b) Flat zone in the point x, $F_x(f)$; (c) Flat zone in the point y, $F_y(f)$; (d) Two adjacent flat zones, i.e, $F_x(f) \cup F_y(f) = \gamma_x (Fx(f) \cup F_y(f))$

In the case of working on the partition the transformations should be operated on the pair (f , P_f) and the element $(f , P_f)(x)$ is taken as the gray level value of the connected component $F_x = \gamma_x (Z_t (f))$. The morphological dilation and erosion applied over the flat zones are given by:

$$\delta(f, P_f)(x) = \max\{ (f , P_f)(y):F_y (f) \in A_x \cup \{ F_x (f) \} \}$$

$$\varepsilon(f , P_f)(x) = \min\{ (f , P_f)(y):F_y(f) \in A_x \cup \{ F_x (f) \} \}$$

The opening and closing on the partition induced by f are:

$$\gamma_\mu(f , P_f)(x)= \delta_\mu(\varepsilon_\mu(f , P_f),P_f)(x)$$

$$\varphi_\mu(f , P_f)(x) = \varepsilon_\mu (\delta_\mu(f , P_f), P_f)(x)$$

Once defined the morphological erosion and dilation on the partition, the morphological gradient, internal gradient and external gradient on the partition are defined as:

$$\text{grad}(f, P_f)(x) = \delta(f, P_f)(x) - \varepsilon(f, P_f)(x) \qquad (3)$$

$$\text{gradi}(f, P_f)(x) = (f, P_f)(x) - \varepsilon(f, P_f)(x)$$

$$\text{gra d e}(f, P_f)(x) = \delta(f, P_f)(x) - (f, P_f)(x) \tag{4}$$

The basic morphological transformations defined in this section enable us to present the morphological toggle mappings of three states in the next section.

2.3 Morphological Toggle Mappings

As was expressed in the introduction, the contrast mappings consist in the selection of some patterns (primitives) for each point of the image in accordance with a proximity criterion. The choosing of the primitives is very important; since the degradation of the output images can be attenuated if the primitives are idempotent transformations as described by Serra [17]. On the other hand, in Mendiola and Terol [11], [12] the morphological toggle mappings on the partition of two and three states with size criteria were proposed. The proximity criterion with size criteria basically permits a different performance of the morphological toggle mappings; hence it is another way of modifying the contrast in an image. As follows the contrast mappings of three states on the partition with size criteria are considered. These toggle mappings are composed by three primitives: opening and closing on the partition and original image (see section 2.2). The proximity criterion ρ(x) (see equations (5)) on the partition takes into consideration the bright and dark regions of the image; and a ratio factor in each point of the image is calculated. The proximity criterion ρ(x) takes its values in the interval [0, 1].

$$\rho(x) = \frac{\varphi_{\mu_1}(f, P_f)(x) - (f, P_f)(x)}{\varphi_{\mu_1}(f, P_f)(x) - \gamma_{\mu_2}(f, P_f)(x)}, \tag{5}$$

Thus, expression (6) establishes a toggle mapping of three states on the partition with size criteria.

$$W^3_{\mu_1,\mu_2,\beta,\alpha}(f, P_f)(x) = \begin{cases} \varphi_{\mu_1}(f, P_f)(x) & 0 \le \rho(\mathrm{x}) < \beta \\ (f, P_f)(x) & \beta \le \rho(\mathrm{x}) < \alpha \\ \gamma_{\mu_2}(f, P_f)(x) & \alpha \le \rho(\mathrm{x}) \le 1 \end{cases}, \tag{6}$$

In the case of working at pixel level, the primitives used are: morphological opening, morphological closing and the original image (see section 2.1). The proximity criterion ρ(x) (see equation (7)) at pixel level takes its values in the interval [0, 1].

$$\rho(x) = \frac{\varphi_{\mu_1}(f)(x) - f(x)}{\varphi_{\mu_1}(f)(x) - \gamma_{\mu_2}(f)(x)}, \tag{7}$$

The toggle mapping of three states at pixel level with size criteria is expressed in the equation (8).

$$W^3_{\mu_1,\mu_2,\beta,\alpha}(f)(x) = \begin{cases} \varphi_{\mu_1}(f)(x) & 0 \le \rho(\mathrm{x}) < \beta \\ f(x) & \beta \le \rho(\mathrm{x}) < \alpha \\ \gamma_{\mu_2}(f)(x) & \alpha \le \rho(\mathrm{x}) \le 1 \end{cases}, \tag{8}$$

The main advantage of working on the partition is that the flat zones of the image will never be broken during their processing; and the generation of new contours into the output image will be avoided. The former situation occurs because the transformations employed are connected. From equations (6) and (8) notice that the size of the structural element is given by the parameters μ_1 and μ_2; while the parameters α and β take values in the interval [0,1]. In this work the size of the parameters μ_1 and μ_2 will be fixed; while the parameters α and β will be changing. The problem is reduced to finding adequate values for the parameters α and β such that the output images present a visual improvement. In Fig. 3, some output images were obtained by the application of formulas (6) and (8). The output images in Figs. 3(b), 3(c) and 3(d) present an

improvement in the contrast; however, we could not say which of these images present the best visual contrast. The next section considers this problem and two quantitative contrast methods will provide an indirect estimation of a contrast measure for each output image.

3 Contrast Measure

The improvement of images after enhancement is often very difficult to measure. In practice, many definitions of the contrast measure are used; for example, see Morrow *et al.* [14], Kim *et al.* [9] and Beghdadi and Negrate [4] . In general terms, contrast refers to the difference in luminance between an object and its surroundings. In psycho visual studies, the contrast C of an object with luminance L against its surrounding luminance L_s is defined as follows [14]:

$$C = \frac{L - L_s}{L_s}$$

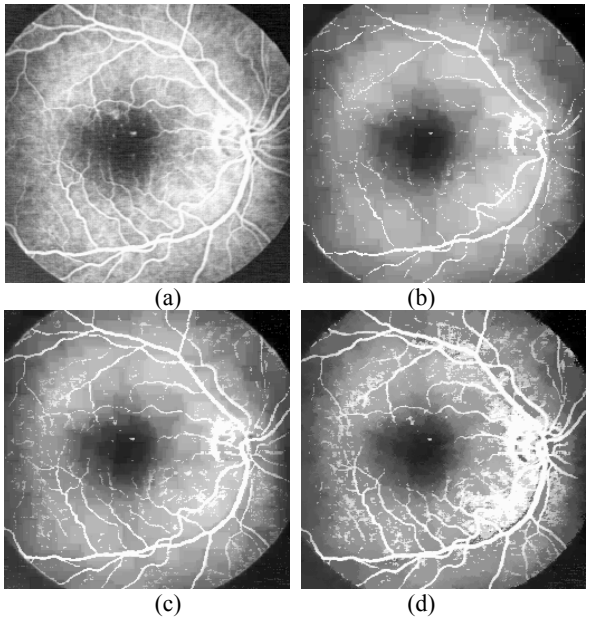

Fig. 3. (a) Original image; (b) Output image with $\mu_1 = 13$, $\mu_2 = 7$, $\alpha = 0.019$ and $\beta = 0.039$ at pixel level; (c) Output image with $\mu_1 = 13$, $\mu_2 = 7$, $\alpha = 0.117$ and $\beta = 0.235$ at pixel level; (d) Output image with $\mu_1=13$, $\mu_2=7$, $\alpha=0.196$ and $\beta=0.392$ on the partition

However, there is not a universal measure which can specify both the objective and subjective validity of the enhancement method [9]. For example, the local contrast proposed by Gordon and Rangayan [6] was defined by the mean grey values in two rectangular windows centered on a current pixel. Beghdadi and Negrate [4] proposed another definition of the local contrast based on the local edge information of the image, in order to improve the method proposed by Gordon and Rangayan [6]. On the other hand, the use of statistical measures of grey level distribution as mea surement of local contrast enhancement (for example, mean, variance or entropy) has not been particularly meaningful when the contrast of the images has been modified. An approach proposed in Morrow *et al*. [14], which has greater consistency than statistical measures, is based on the contrast histogram. In Agaian *et al.* [1] an interesting method was proposed in order to obtain a quantitative measure of image enhancement. Basically the maximum intensity and minimum intensity inside the block were analyzed to calculate the measure of the enhancement. Starting from this idea, we introduce two methods allowing us to determine which image has a good visual contrast in a set of images. The first of them employs a physical concept denominated difference of contrast and the second one makes use of the gradient luminance concept. Both methods rely on some enhancement parameters.

3.1 Model to Evaluate the Contrast Quality Based on the Difference of Contrast

In Jain [8] the Weber law was expressed by means of a logarithm expression; i.e.:

$$C = a_1 + a_2 \log L \tag{9}$$

Where C is called the contrast, L the luminance, a_1 and a_2 two constants. If $a_1=0$, the equation (9) is written as:

$$C = a_2 \log L \tag{10}$$

The difference of contrast (G) considering a_2 fixed can be calculated from equation (10) and is expressed by:

$$G = C_i - C_j = a_2 \log\left(\frac{L_i}{L_j}\right) \tag{11}$$

An indirect measure of the difference of contrast G, can be obtained from equation (11) if the luminance L is substituted by the gray level intensity of function f. Considering $L_i \approx f_s$ and $L_j \approx f_o$, where f_o and f_s belong to the domain of definition of f, denoted by D_f. Expression (11) is written as:

$$G = a_2 \log\frac{f_o}{f_s} \qquad f_o \neq f_s \quad \text{with } f_o, f_s \in D_f \tag{12}$$

In our particular case, $f_o = I_{max}(x)$ and $f_s = I_{min}(x)$; where $I_{max}(x)$ and $I_{min}(x)$ represent the maximum and minimum intensity values taken from one set of pixels contained in a window (B) of elemental size (3×3 elements), and $x \in D_f$. Notice that the window corresponds to the structuring element B. The sum of the values of G (see equation (12)) for each pixel of an image f of size N×M is denoted as GI, and the formulation is written in equation (13). For the sake of simplicity; let us consider $I_{max}(x) = \max\{f(x+b): b \subseteq B\}$ and $I_{min}(x) = \min\{f(x+b): b \subseteq B\}$; $x \in D_f$. Then:

$$GI = \sum_{x \in Df} a_2 \log\frac{I_{max}(x)}{I_{min}(x)} \tag{13}$$

Where $I_{max}(x)$ and $I_{min}(x)$ values correspond with the morphological dilation and erosion defined by the order-statistical filters [10]. Thus, equation (13) can be expressed as:

$$GI = \sum_{x \in Df} a_2 \log\frac{\delta(f)(x)}{\varepsilon(f)(x)} \tag{14}$$

By some algebraic steps the equation (14) is rewritten as follows:

$$GI = a_2 \sum_{x \in Df} \left[\log(\delta(f)(x)) - \log(\varepsilon(f)(x))\right] \tag{15}$$

The morphological erosion and dilation commute with anamorphoses [18], [19], therefore:

$$\varepsilon(\log f) = \log\varepsilon(f) \text{ and } \delta(\log f) = \log\delta(f) \tag{16}$$

By applying expressions (16) and (1), equation (15) can be written as:

$$GI = a_2 \sum_{x \in Df} \text{grad}(\log f(x)) \tag{17}$$

Note that the morphological gradient (see equation 1) employed in this case is at pixel level; however equation (3) must be considered if the analysis is carried out on the partition. In equation (17) the a_2 value has not been calculated; but in accordance with the Weber law, the constant a_2 has been found to be 50. The Weber law is expressed as [8]:

$$C=50\log L$$

Consequently, for L=100, C =100. If the maximum intensity value in the analyzed images is 255, the value of a_2 is calculated as follows:

$$a_2\log 255 = 50\log 100 \text{ then } a_2 \approx 41.55 \tag{18}$$

Taking the value of a_2 encountered in (18); the final expression of GI is given by equation (19)

$$GI = 41.55 \sum_{x \in Df} \text{grad}(\log f(x)) \tag{19}$$

Equation (19) indicates that the measure of GI is given by the morphological gradient acting on a space visually improved by the logarithmic law. The following steps enable us to determine the best values of GI and consequently the images corresponding to these values:

Step 1.-Calculate and graph the *GI values vs. parameters* for a set of images.
Step 2.- Obtain the *global maximum* or the *minimum with greater altitude* of the graph *GI values vs. parameters*. The image with good visual contrast will be associated to the *global maximum* or *minimum with greater altitude* contained within a subset of GI values where their behavior is almost constant.

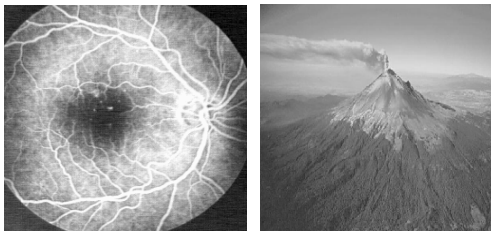

(a) (b)

Fig. 4. (a),(b) Original images

The fact of choosing a subset of GI values where their behavior is almost constant obeys to the next two situations: a) A constant interval of GI values indicates that the internal structures of the image present a stable behavior. In other words, the internal structures of the image do not change considerably when the enhancement filter is applied. In this interval the output images will be smooth. b) In smooth images, the signal to noise ratio is low, making well defined edges; these edges are perceived as having more detail or signal.

Images with high signal-noise quotients are perceived as agreeable to the eye; however, sharp shadow edges or luminance discontinuity may have high values, but this not necessarily means a good contrast. For example: if an input image is processed with a contrast enhancement transformation producing a great degradation in the output image, then higher GI values can produce an output image without good visual contrast. In consequence the election of the parametric values controlling directly the contrast transformations must be done with care in order to avoid the problems mentioned above. In order to illustrate the performance of this quantitative contrast method, the images in Fig. 4 will be processed; subsequently steps 1 and 2 will be applied. This analysis is achieved at pixel and on the partition level.

The parameters $\mu_1 = 13$ and $\mu_2 = 7$ where used in equations (5), (6), (7) and (8) as fixed parameters. While α and β varied in the close interval [0, 1], in such a way that 27 output images were generated. For each output image generated, the values of GI were calculated at pixel and on the partition level; and their respective values may be found in Table 1. By applying step 1; the GI values are calculated and the graphs of these values are presented in Fig. 5. Note that each graph has a 3D representation considering the parameters α, β and GI values. By considering a process at pixel level and using equations (7) and (8), graphs in Figs. 5(a) and 5(b) are obtained; while the graphs in Figs. 5(c) and 5(d) correspond to the im-

ages processed by means of equations (5) and (6). Step 2 allows the determination of the best parameters associated with the output images having a good visual contrast. Such parameters are obtained from Table 1 and they are presented in Table 2 (analysis at pixel level) and Table 3 (analysis on the partition). The images presenting a good visual contrast in accordance with the model employed are shown in Fig. 6. The four output images of Fig. 6 present a good visual contrast with respect to the model utilized;

Table 1. GI values of the output images generated from: (a) Fig. 4(a) at pixel level; (b) Fig. 4(b) at pixel level; (c) Fig. 4(a) on the partition; (d) Fig. 4(b) on the partition

Nº of image	α	β	(a)	(b)	(c)	(d)
1	0	0	82962,9417	35591,59	146662,89	41918,27
2	0.019	0.039	273979,466	144007,869	284220,43	128697,73
3	0.039	0.078	293499,884	171921,029	312527,7	160493,54
4	0.058	0.117	317949,041	205339,82	337984,8	195917,78
5	0.078	0.156	346806,781	248234,06	355443,14	234100,82
6	0.098	0.196	358912,63	294282,71	370028,45	277826,526
7	0.117	0.235	396587,99	333197,3	388471,4	323543,51
8	0.137	0.274	428753,15	368931,92	408302,11	364771
9	0.156	0.313	443631,32	398006,768	423133,09	403370,47
10	0.176	0.352	468914,5	415230,31	467319,3	424762,13
11	0.196	0.392	479843,94	421780,8	476224,84	433270,58
12	0.215	0.431	492983,99	416898,12	523370,68	432317,1
13	0.235	0.470	501461,04	406119,11	525066,92	423159,82
14	0.254	0.509	496030,78	387869,12	525630,05	408050,29
15	0.274	0.549	499873,05	368238,3	537924,73	388620,037
16	0.294	0.588	486847,9	345637,99	486847,9	366612,47
17	0.313	0.627	474190,73	328031,82	503673,41	350406,62
18	0.333	0.666	473306,242	315317,69	506907,27	334869,87
19	0.352	0.705	461409,43	291308,64	478033,95	318783,27
20	0.372	0.745	454945,199	293330,08	480810,01	308272,95
21	0.392	0.784	442201,39	287242,68	469884,17	299586,61
22	0.411	0.823	431201,87	282033,511	468481,8	293748,98
23	0.431	0.862	424879,65	277140,772	470592,42	289589,53
24	0.450	0.901	415317,92	272347,36	445731,16	284514,16
25	0.470	0.941	410222,89	266812,026	415896,31	279230,6
26	0.490	0.98	409489,92	260026,489	410390,94	274127,82
27	0.509	1	402560,48	250689,29	408945,03	265855,95

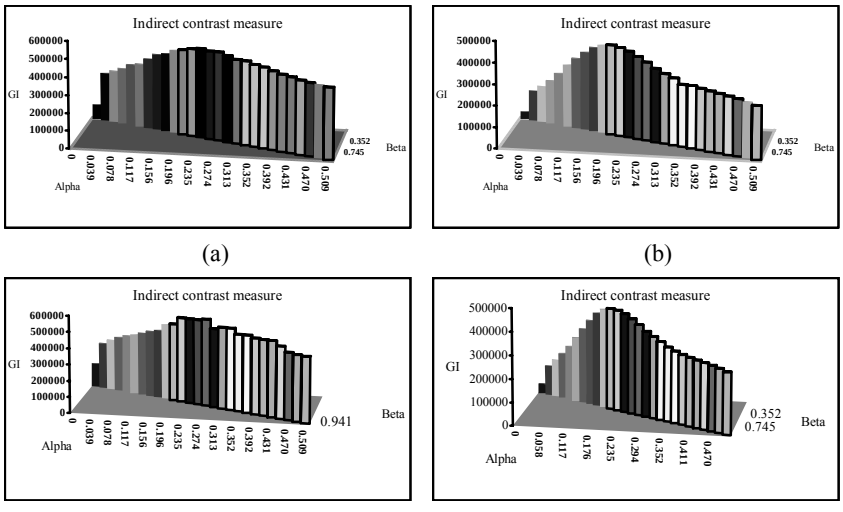

Fig. 5. (a),(b),(c),(d) Respective graphs of the GI values obtained from Table 1

Table 2. Selection of the maximum or minimum obtained from the graphs of Figs. 5 (a) and 5(b). In this case the images were processed at pixel level

Figures	Global maximum	Minimum with greater altitude	Maximum or minimumin accordance with step 2	Image selected
Fig 2(a)	468914,5	479843,94	479843,94	Nº of image:14
Fig.2(b)	421780,8	291308,64	421780,8	Nº of im-age:11

Table 3. Selection of the maximum or minimum obtained from the graphs of Figs.5 (c) and 5(d). In this case the images were processed on the partition

Figures	Global maximum	Minimum with greater altitude	Maximum or minimum in accordance with step 2	Image selected
Fig 2(c)	537924,73	486847,9	537924,73	Nº of image:15
Fig.2(d)	433270,58	-	433270,58	Nº of image:11

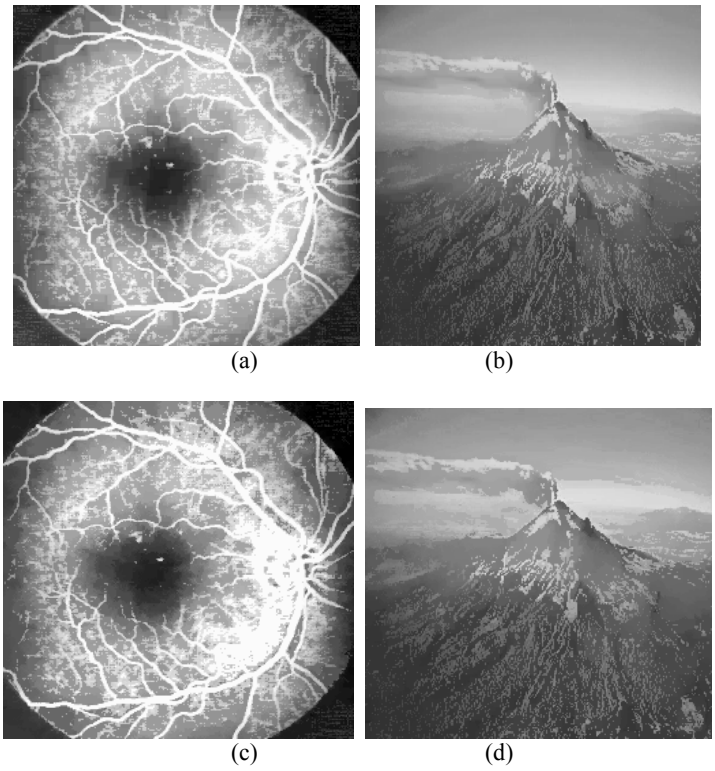

(a) (b) (c) (d)

Fig. 6. Output images with the parameters obtained from Table 2 and Table 3; (a),(b) Output images processed at pixel level; (c),(d) Output images processed on the partition

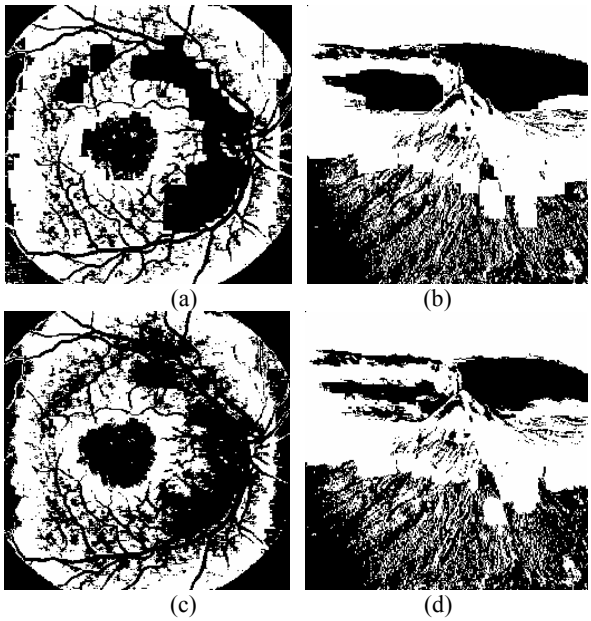

Fig. 7. Threshold of the images in Figure 6, (a) Fig. 6(a) between 90-187 sections; (b) Fig. 6(b) between 84-173 sections; (c) Fig. 6(c) between 90-187 sections; (d) Fig. 6(d) between 84-173 sections

However, the flat zones of the output images processed at pixel level will be broken, which does not occur when the images are processed on the partition. In order to show this effect, the threshold for each image of Fig. 6 is obtained and the results can be observed in Fig. 7. Compare the images of Fig. 7(a)-7(b) with the images of Fig.7(c)-7(d) and note that the shape of the structural element appears in the image when these are processed at pixel level.

This fact let us determine that the images computed on the partition will have a better behavior than those obtained from a pixel level treatment. The measure of the contrast in the images not necessarily indicates a good visual contrast. By analyzing formula (13) note that a greater difference between I_{max} (x) and I_{min}(x) does not correspond with what we see; since higher GI values can be obtained for different parameters, but the output images associated with these parameters probably have not a good visual contrast. This fact makes us to find the regions where GI values present an almost constant behavior into the graphs in order to detect the best parameters. The traditional way of studying structures sizes constituting the image is by means of the granulometric study of the image [16]. In Fig. 8 the curves for determining the structures sizes of the images 6(b) and 6(d) are shown for the opening case. Although these curves do not correspond with the granulometric definition, the form of the curves is similar to those of granulometric density. The curves in Fig. 8 were obtained for sizes of the structural element (μ) in the interval [1,20] and each value was calculated over the integral of the image $\gamma_{\mu}(f , P_f)- \gamma_{\mu+1}(f , P_f)$ in the partition case and $\gamma_{\mu}(f)- \gamma_{\mu+1}(f)$ at pixel level. Note that at pixel level the graph in Fig. 8(a) detects a great variation in sizes; while in the curve of the Fig. 8(b) several flat zones have been merged and a smooth curve is obtained. In the case of image 6(d) two important accumulated regions have been detected in the graph of Fig. 8(b).

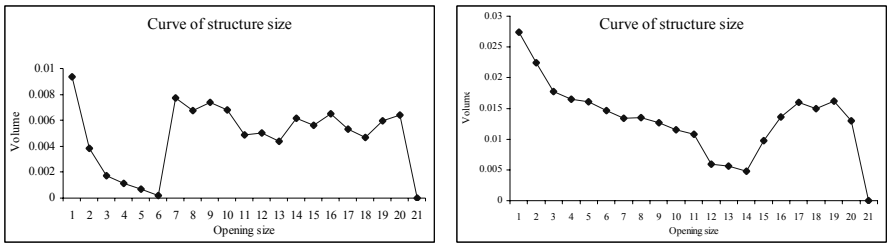

(a) (b)

Fig. 8. (a) Integral (Volume) on the image $\gamma_{\mu}(f)- \gamma_{\mu+-1}(f)$, (b) Integral (Volume) on the image $\gamma_{\mu}((f , Pf))- \gamma_{\mu+1}((f , Pf))$

Until now, the main idea to obtain well contrasted images from a visual point of view, establishes that the smoothing of the images will produce well defined contours. However, the measure of the GI values does not involve the contours of the image. Therefore another method to quantify the contrast is proposed; where the contours of the image are taken into account.

3.2 Contrast Measure Based on the Analysis of Image Edges

Given a two-dimensional luminance distribution across a surface, the luminance gradient is defined as [2]:

$$\frac{\Delta L}{\Delta x} = \left| \frac{L_b - L_a}{b - a} \right|$$

Where L_a and L_b are the luminances at two closely spaced points *a* and *b* on the surface, and where the points are separated by a distance $\Delta x = b - a$. (The absolute value is necessary to eliminate any directional dependence.) When $\Delta x \to 0$:

$$\left. \frac{\Delta L}{\Delta x} \right|_{lim\ x \to 0} = \left| \frac{dL}{dx} \right|$$

Changes in luminance are associated with the contours of the image, since they produce changes in the scene. One transformation that enables us to work directly with the contours of the image is the morphological external gradient (see equation 2). This gradient expression is used in order to have an indirect measure of the variations of the contras (VLG) into a window B. For the sake of simplicity; let us consider $maxgrade(x) = \max\{grade(x+b): b \in B\}$ and $mingrade(x) = \min\{grade(x+b): b \in B\}$; where *x* belongs to the domain of definition of f; denoted by D_f. The VLG expression is given as follows:

$$VLG = \sum_{x \in Df} \left[max\ \text{gra}\ de(x) - min\ \text{gra}\ de(x) \right] \qquad (20)$$

Where maxgrade(x) represents the maximum intensity value of the external gradient and mingrade(x) the minimum intensity value of the external gradient. These values are taken from one set of pixels contained in a window (B) of elemental size (3×3 elements). Expression (4) for the external gradient must be considered in the case of working on the partition. Again a set of output images will be analyzed with the objective of knowing which output contrasted image presents good visual contrast. The idea of this second quantitative contrast method consists in the selection of the best parameters associated with some value of VLG obtained from the graph *VLG vs. parameters*. The analysis of the graphs will be focused mainly on the maxima and minima of the graphs, since they are associated with substantial changes in intensity. For the global maximum of the graphs, the contrast of the images will be higher; while the global minimum will produce a smooth contrast. The steps 3, 4 and 5 will be employed for the selection of local maximum and minimum producing good visual contrast.

Step 3.-Calculate and draw the graph *VLG values vs. parameters* for a set of output enhanced images.

Step 4.- A smooth visual contrast will correspond to the value of VLG associated with the *global minimum* or *maximum with smaller altitude* in the graph of *VLG values vs. parameters*.

Step 5.- A higher visual contrast will correspond to the value of VLG associated with the *global maximum* or the *minimum with greater altitude* in the graph of *VLG values vs. parameters*.

Step 6.-An intermediate visual contrast will correspond to the value of VLG associated with any local maximum or local minimum not considered in steps 4 and 5.

In order to illustrate the performance of this second contrast method, the images in Fig. 4 were analyzed. These images were processed at pixel level with equations (7) and (8); the analysis on the partition was done with equations (5) and (6). The parameters $\mu_1 = 13$ and $\mu_2 = 7$ in the equations (5), (6), (7) and (8) were fixed; and the variable parameters α and β took their values in the interval [0, 1]. Step 3 establishes that VLG values must be calculated and plotted. In Table 4 the VLG calculated values are presented.

The maximum or minimum for each processed image can be obtained from Table 4 and the graphs are presented in Fig. 9. The analysis of the maximum and minimum corresponding to each output image is summarized in Table 5 (analysis at pixel level) and Table 6 (analysis at partition level) in agreement with steps 4 and 5. The set of output images related to the parameters of Tables 5 and 6 are shown in Fig. 10.

Table 4. VLG values of the output images generates from: (a) Fig. 4(a) at pixel level, (b) Fig. 4(b) at pixel level, (c) Fig. 4(a) on the partition, (b) Fig. 4(b) on the partition

Nº of image	α	β	(a)	(b)	(c)	(d)
1	0	0	178062	102345	226833	90075
2	0.019	0.039	856950	382502	852736	369460
3	0.039	0.078	1001434	433160	967186	431527
4	0.058	0.117	1092674	488086	1116680	517252
5	0.078	0.156	1163136	541931	1224875	573834
6	0.098	0.196	1252704	593671	1338330	627690
7	0.117	0.235	1335568	637264	1401583	676019
8	0.137	0.274	1427302	688872	1493208	716025
9	0.156	0.313	1491286	723719	1538241	749970
10	0.176	0.352	1542954	766278	1594667	794928
11	0.196	0.392	1599556	812012	1651967	845687
12	0.215	0.431	1636148	851577	1688989	890145
13	0.235	0.470	1664972	887289	1693407	925872
14	0.254	0.509	1691804	912013	1695790	956024
15	0.274	0.549	1696840	928967	1679666	967923
16	0.294	0.588	1687766	940656	1655937	972618
17	0.313	0.627	1665154	935399	1622253	965099
18	0.333	0.666	1636698	924885	1583523	952551
19	0.352	0.705	1602930	905318	1524559	933482
20	0.372	0.745	1593142	883827	1500465	916387
21	0.392	0.784	1569358	865932	1463979	895523
22	0.411	0.823	1551284	849744	1442468	875836
23	0.431	0.862	1539342	836728	1411789	861055
24	0.450	0.901	1526936	823852	1403806	847619
25	0.470	0.941	1523970	811735	1395297	835626
26	0.490	0.98	1528378	803113	1395838	832581
27	0.509	1	1528738	800563	1403214	835087

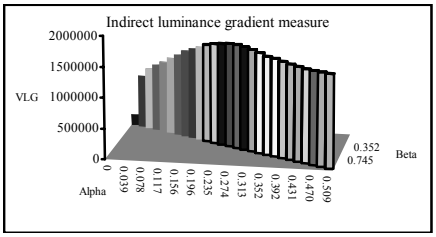

(a)

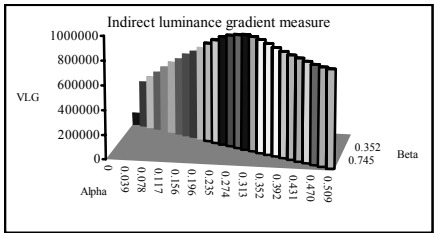

(b)

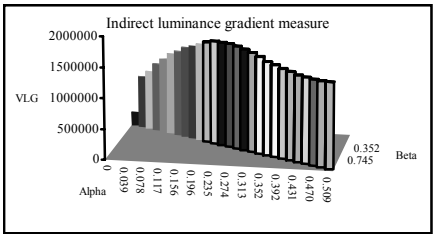

(b)

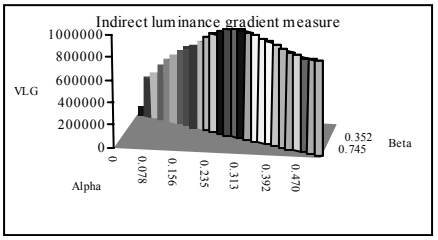

(d)

Fig. 9. (a),(b),(c),(d) Respective graphs of the VLG values obtained from Table 2

Table 5. Selection of the maximum and minimum obtained from the graphs of Figs. 9(a) and 9(b). In this case the images were processed at pixel level

Figure	Global maximum	Global minimum	Nº of image
2(a)	1696840	1395297	15, 25
2(b)	940656	-	16

Table 6. Selection of the maximum and minimum obtained from the graphs of Figs.9 (c) and 9(d). In this case the images were processed on the partition.

Figure	Global maximum	Global minimum	Nº of image
2(a)	1695790	1395297	14, 25
2(b)	972618	832581	16, 26

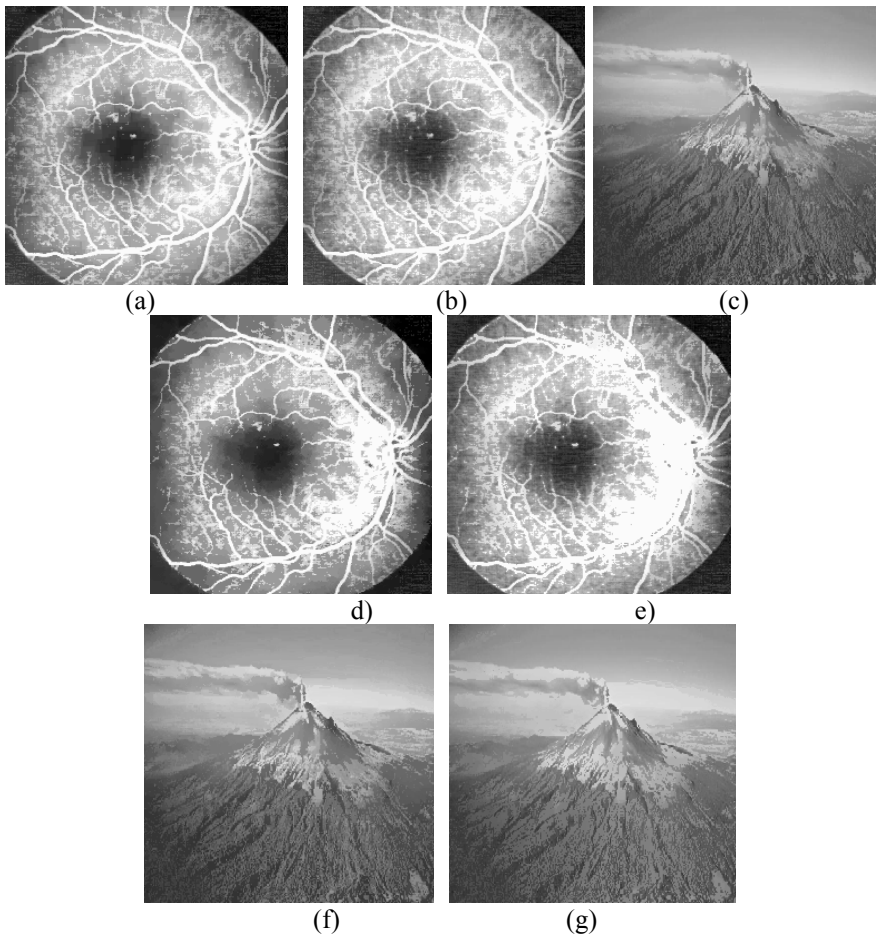

Fig. 10. (a),(c) Output images with a higher visual contrast, at pixel level; (d),(f) Output images with a higher visual contrast, on the partition; (b) Output image with a smooth visual contrast at pixel level; (e),(g) Output images with smooth visual contrast on the partition

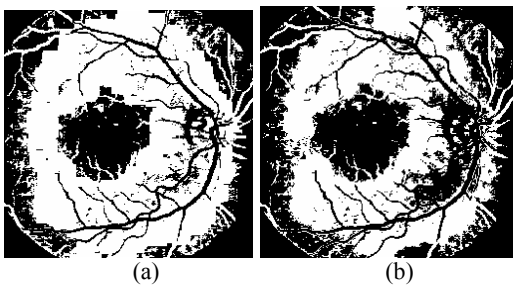

Fig. 11. (a) Threshold of Fig. 10(a) between 139-245 sections; (b) Threshold of Fig. 10(d) between 139-245 sections

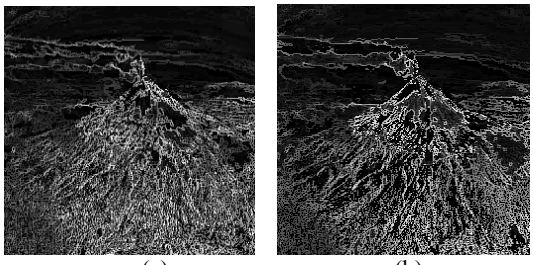

(a) (b)

Fig. 12. In both images the contours were multiplied by 4, (a) Internal gradient on the partition of the image in Fig. 10(f); (b) Internal gradient on the partition of the image in Fig. 10(g)

The output images in Fig. 10(a),10(c),10(d) and 10(f) complying with step 5 present a high visual contrast. While the images in Fig. 10(b),10(e) and 10(g) have a smooth visual contrast in agreement with step 4. The output images processed on the partition present a better behavior that those processed at pixel level, since they have been processed by means of a connected transformation; in consequence the flat zones of the images will never be broken. Observe this behavior in Fig. 11. The main difference among the output contrasted images obtained in Fig, 10 are the contours of the images. Smooth images will present more defined contours; such images were obtained from the global minimum; whereas images associated with the global maximum will present sharp contours related to high intensity zones of the image. As an example Fig 12 describes this circumstance. In this case the internal gradient on the partition was obtained for the images in Figs.10 (f) and 10(g). In Fig. 12(b) several flat zones were merged and the contours of this image are more defined than those contours within the image in Fig. 12(a). The neighboring pixels surrounding the contours in the images of Figs. 10(a), Fig.10(c), 10(d) and 10(f) are characterized as suffering important changes of intensity, therefore they are classified as high contrast images; rather the images of Fig. 10(b), 10(e) and 10(g) which present a smooth contrast. This behavior can be understood by comparing the histograms of the internal gradient of these images. One example is given in Fig. 13.

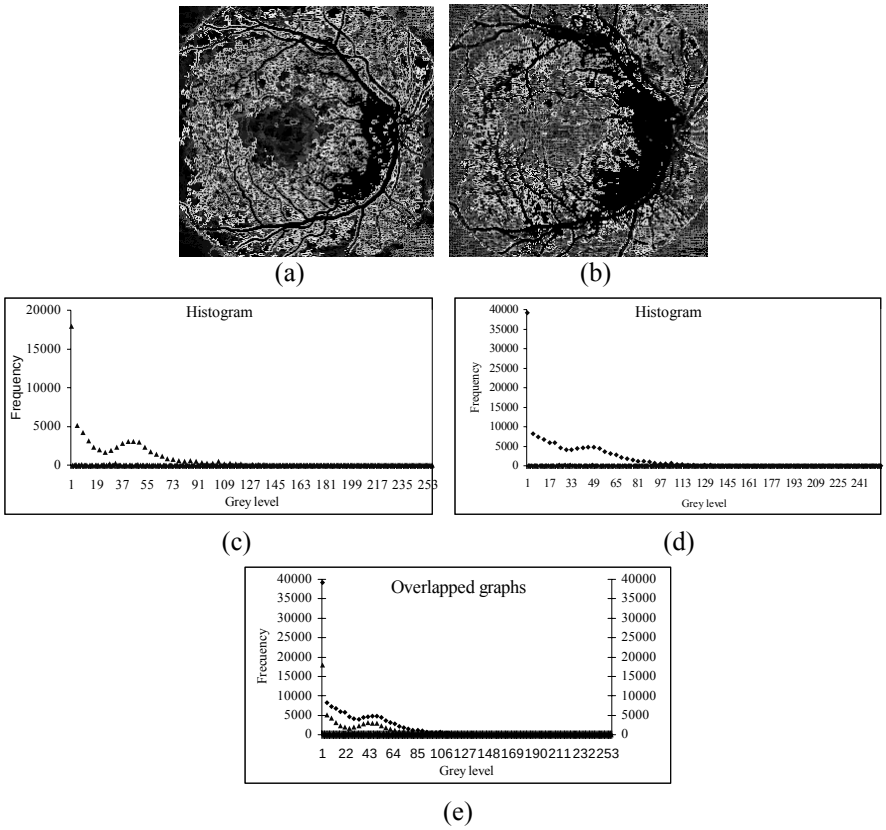

(a) (b) (c) (d) (e)

Fig. 13. (a) Gradient on the partition of the images in Fig. 10(d); (b) Gradient on the partition of the images in Fig. 10(e); (c) Histogram of the internal gradient on the partition of the image in Fig. 10(d), (d) Histogram of the internal gradient on the partition of the image in Fig. 10(e); (e) Overlapped graphs

In Fig. 13(a) and 13(b) the internal gradient on the partition of the images in Fig. 10(d) and 10(e) are presented. The histogram of the image in Fig. 13(a) is shown in Fig. 13(c). This histogram is associated with a high visual contrast. In the case of a smooth contrast, the histogram is given in Fig 13(d); here the histogram of the internal gradient on the partition of the image in Fig. 10(e) is obtained. The histogram of Fig. 13(c) presents more variations than the one in Fig. 13(d); which explains the high contrast in Fig.10 (d). Notice that the frequency for the values in the histogram of Fig. 13(d) is greater than the one in histogram of Fig. 13(c). This fact is due to the merging of several flat zones during the image processing, resulting in a better contrast (see Fig. 10(e)). In Fig. 13(e), graphs 13 (c) and 13(d) are overlapped in order to have a better appreciation of this situation.

The output images obtained through both quantitative contrast methods present some important differences; the first method analyzes all contours in a general way; while the second method analyzes only the regions where there are important changes in the contours. Therefore each one of these quantitative contrast methods must be applied taking into consideration these differences.

4 Conclusion

Two quantitative contrast methods have been proposed in order to determine the output images associated with a good visual contrast. In accordance with the analyzed examples, the behavior of the output contrasted images is better when they are processed on the partition by means of connected transformations. Finally the quantitative contrast methods presented are simple to apply and design, rendering them practical.

Acknowledgments

The author Jorge D. Mendiola Santibañez would like to thank CONACyT México for the financial support. The author I. Terol would like to thank Diego Rodrigo and Darío T.G. for their great encouragement. This work was partially funded by the government agency CONACyT (Mexico) under the grant 41170.

References

1. **Agaian, S.S., Panetta, K., and Grigoryan, A.M.:** Transform-Based Image Enhancement Algorithms with Performance Measure, IEEE Transactions on Image Processing, 10(2001) 367-382.
2. **Ashdown, I.:** Luminance gradients: photometric analysis and perceptual reproduction, Journal of the Illuminating Engineering Society, 25 (1996) 69-82.
3. **Barten, P. G. J.:**Physical model for the contrast sensitivity of the human eye, in Proceedings of SPIE, 1666 (1992) 57-72.
4. **Beghdadi, A. and Negrate, A. L**.: Contrast enhancement technique based on local detection of edges, Comput. Vis., Graph., Image Process., 46 (1989) 162–274.
5. **Blommaert, F. J. J. and Martens, J**.: An object-oriented model for brightness perception, Spatial Vision, 1, (1990) 15-41.
6. **Gordon ,R., and Rangayyan, R.M.:** Feature enhancement of film mammograms using fixed and adaptative neighbourhoods, Appl. Opt., 23, (1984) 560-564.
7. **Horn, B. K. P**.:Determining lightness from an image, Computer Graphics and Image Processing, 3, (1977) 277-299.
8. **Jain, A. K.,** Fundamentals of Digital Image Processing. Englewood Cliffs, NJ: Prentice Hall (1989).
9. **Kim, J. K., Park, J. M., Song, K. S., and Park, H.W**.: Adaptive mammo-graphic image enhancement using first derivative and local statistics, IEEE Trans. Med. Imag., 16 (1997) 495–502.
10. **Maragos P. and Schafer R. W**.: Morphological Filters-Part I: Their set-theoretic analysis and relations to linear shift-invariant filters, IEEE Trans. Acoust., Speech, Signal Processing, **35** (1987) 1153-1169.
11. **Mendiola-Santibañez, J.D. and Terol-Villalobos, I. R**.:Morphological contrast enhancement using connected transformations, in Proceedings of SPIE, 4667 (2002) 365-376.
12. **Mendiola-Santibañez, J.D and Terol-Villalobos, I. R**., "Mapeos de Contraste Morfológicos sobre Particiones Basados en la Noción de Zona Plana" Computación y Sistemas, 6,(2002) 25-37.
13. **Meyer, F. and Serra, J.,** : Activity Mappings, Signal Processing,16, (1989) 303-317.
14. Morrow, W. M., Paranjape, R. B., Rangayyan, R. M., and De-sautels, J. E. L.:Region-based contrast enhancement of mammograms, IEEE Trans. Med. Imag., 11, (1992) 392–406.
15. **Peli, E**.:Contrast in Complex Images, J. Optical Society of America , 7, (1990) 2032-2040.

16. **Serra, J**.: Image Analysis and Mathematical Morphology, J. Serra, Ed., Vol. I, Academic Press, New York (1982).
17. **Serra, J**.: Toggle Mappings, Technical report N-18/88/MM, Centre de Morphologie Mathematique, ENSMP, Fontainebleau, France (1988).
18. **Serra, J.:** Image Analysis and Mathematical Morphology, J. Serra, Ed., Vol. II, Academic, New York (1988).
19. **Serra, J**.: Anamorphoses and function lattices, in Mathematical Morphology in Image Processing, E. Dougerty, ed., Dekker, New York (1992).
20. **Serra, J**.: Morphological filtering: An overview, Signal Processing, 38 (1993) 3-11.
21. **Stockham, T. G. Jr.:** Image processing in the context of a visual model, Proc. IEEE, 60, (1972) 828-842.
22. **Terol-Villalobos, I. R**.: Nonincreasing filtres using morphological gradient criteria, Optical Engineering, 35 (1996) 3172-3182.
23. **Terol-Villalobos, I. R. and Cruz-Mandujano, J.A**.: Contrast enhancement and image segmentation using a class of morphological nonincreasing filters, Journal of Electronic Imaging, 7 (1998) 641-654.
24. **Terol-Villalobos, I. R**.: Toggle mappings and some related transformations: A study of contrast enhancement", in Mathematical Morphology and Its Applications to Image and Signal Processing, H.J.A.M. Heijmans and J.B.T.M. Roerdink , Eds., Kluwer Academic Publishers, The Netherlands (1998) 11-18.
25. **Terol-Villalobos, I.R**.: Morphological Image Enhancement and Segmentation, in Advances in Imaging and Electron Physics, Editor Peter W. Hawkes, Vol. 118, Chapter 4, Academic Press (2001) 207-273.

Jorge D. Mendiola-Santibañez. *He received the B.S. degree in Electronic engineering from the Benemérita Universidad Autónoma de Puebla, Mexico, his M.S. degree in Electronics from INAOE (México). He received his PhD. degree from the Universidad Autónoma de Querétaro (México). He is currently a reaseacher of Universidad Autónoma de Querétaro (Querétaro, México). His research interests include morphological image processing, and computer vision.*

Iván R. Terol-Villalobos*. He received his BSc degree from Instituto Politécnico Nacional (I.P.N. México), his MSc degree in Electrical Engineering from Centro de Investigacion y Estudios Avanzados del I.P.N. (México), and a DEA in Computer Science from the University of Paris VI (France). He received his PhD degree from the Centre de Morphologie Mathématique, Ecole des Mines de Paris (France). He is currently a researcher of Centro de Investigación y Desarrollo Tecnológico en Electroquímica (Querétaro, México). His main current research interests include morphological image processing, morphological probabilistic models and computer vision.*